

Modeling Soil–Foundation Interaction and Beyond

Subhadeep Banerjee

Abstract This paper presents a study on seismic soil–pile installation using numerical modeling in conjunction with centrifuge model studies. The numerical analyses were conducted using ABAQUS with a hypoelastic constitutive model for the clay. Numerical analyses were used to extend the range of soil, pile, and ground motion parameters which could not be studied in centrifuge. The dimensionless parameters involving the major parameters such as pile modulus, soil modulus, slenderness ratio, natural frequencies of clay layer and pile-raft, superstructure mass, density of the soil and peak ground acceleration were obtained from the parametric studies. The relationships for the amplification of ground motions and the maximum bending moment in the pile were developed based on regression of the numerical data.

Keywords Earthquake · Piles · Clays · Amplification · Bending moment

1 Introduction

Many major cities such as Shanghai, Bangkok, Mumbai, Kuala Lumpur, Jakarta, and Singapore are built overlying soft problematic soils. As a result, many important inland and offshore structures such as bridges, port and harbors, tall structures like water tanks, chimney are supported on pile foundations to achieve the required load carrying capacity. In such situations, the response of pile and surrounding soil subjected to cyclic lateral loadings such as earthquakes, sea-waves, blasts is an important factor affecting the integrity of infrastructures. There is a significant history of observed soil–pile interaction under cyclic loading, has often resulted in pile and/or structural damage or failure. For instance, the potential significance of damage to piles was clearly demonstrated during the 1995 Kobe earthquake and more recent 2005 Sumatran earthquake.

S. Banerjee (✉)
IIT Madras, Madras, India
e-mail: subhadeep@iitm.ac.in

Since early 1970s various analytical procedures (Novak 1974; Dobry 1982; Shen and Teh 2004) and numerical simulations (Zhang et al. 2000; Nikolaou et al. 2001) have been developed for soil–pile interaction. In general, different types of constitutive relationships ranging from linear elastic to complex nonlinear elasto-plastic models were adapted to model stress–strain behavior of soil. However, most of those analytical or numerical techniques are often restricted to relatively idealized conditions. In view of that, the present paper details a few three-dimensional numerical analysis and parametric studies carried out on piles embedded in problematic soils.

2 Numerical Simulations of Seismic Clay–Pile–Raft Interaction

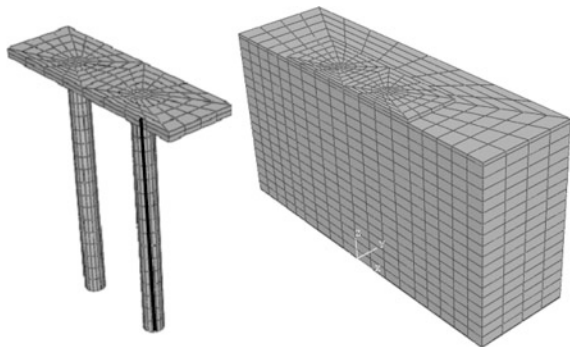
The first study describes the details and results of seismic effects on fixed-head, end-bearing piles installed through soft clay, using numerical modeling in conjunction with centrifuge studies. The numerical analyses were conducted using ABAQUS 6.7.1. The numerical analyses were extended to a range of soil, pile, and ground motion parameters to establish a framework for estimating earthquake-induced bending moments and amplification of seismic waves in fixed-head piles.

2.1 Numerical Model

The soil–pile–raft system was analyzed using a half-model consisting of 20-noded brick elements, Fig. 1.

The results of centrifuge experiments were used to validate the numerical simulations. Experiments were conducted using a laminar box cum shaking table assembly mounted on the NUS geotechnical centrifuge. The earthquake shaker consists of a laminar box seated on top a hydraulic actuator. To simulate laminar

Fig. 1 3-D half-model for soil–pile–raft analysis



movements, linear multi-point constraints were applied to the two vertical faces normal to the input motion, so that nodes at opposite ends of the domain and at the same depth move in unison with each other. In addition, the nodes on the vertical plane of symmetry were restrained against any horizontal displacements in the direction normal to this plane. The remaining three vertical faces, as well as the base of the mesh, were restrained against vertical motion.

The model pile-raft system comprises of four cylindrical model piles, each 260 mm long, connected to a 250 mm long \times 150 mm wide \times 10 mm thick steel plate which acts as a raft. The four piles are bolted to the steel plate so that the pile-head condition may be considered to be fixed. Three types of model piles, three different materials and of diameters 18 mm (0.9 m prototype), were used (Table 1). Superstructural masses were simulated by steel plates bolted on top of the raft, which impose a uniformly distributed load on the surface of the pile cap. In this study, up to six steel plates, each 1.9 kg mass, were added on the pile-raft system (In the prototype, Mass-1: 368 tonnes, Mass-2: 605 tonnes, and Mass-3: 863 tonnes).

The engineering properties of the kaolin clay as reported by Goh (2003) were adopted in the study and are shown in Table 2. The clay beds were prepared by consolidating clay slurry in the laminar box under 1 g preloading, followed by 50 g consolidation. The soft clay behavior was characterized using ABAQUS in-built hypoeastic stress–strain model that exhibits nonlinear, but reversible, stress–strain behavior even at small strains. Physically, the model considers the degradation of shear modulus of soil with respect to increasing shear strain within the soil mass.

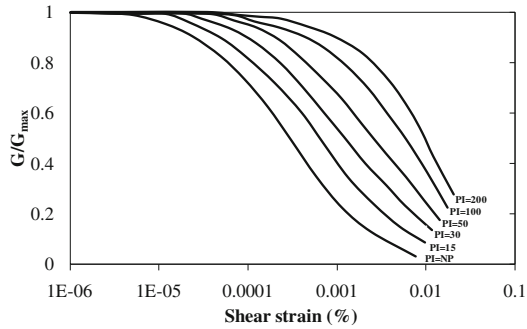
Table 1 Different types of piles used in the numerical simulations

Pile material	Length (m)	Dia. (m)	Slenderness ratio (l/r)	EI (kN/m^2)
Hollow stainless steel	13	0.9	28.89	3,545,002
Hollow stainless steel filled with PCC	13	0.9	28.89	4,285,785
Solid stainless steel	13	0.9	28.89	10,308,351

Table 2 Geotechnical properties of kaolin clay (After Goh 2003)

Properties	Range
Bulk unit weight (kN/m^3)	16
Water content (%)	66
Liquid limit (%)	80
Plastic limit (%)	40
Cohesion (kPa)	30
Young's modulus (MPa)	198
Compression index	0.55
Recompression index	0.14
Coefficient of permeability (m/s)	1.36×10^{-8}

Fig. 2 Modulus reduction curves proposed by Vucetic and Dobry (1991)



Vucetic and Dobry (1991) presented sets of design curves for variation of modulus reduction with strain amplitudes for different plasticity index (Fig. 2). These well-established data sets were used to derive the values of shear modulus corresponding to a specified strain and used as inputs to the constitutive model. The equivalent viscous damping of 10% is used in the analysis.

The input base motions were synthesized from ground motion response spectra of far-field Sumatran earthquakes measured by seismological stations in Singapore (Yu and Lee 2002; Banerjee et al. 2007) and are representative of the bedrock motions in Singapore due to far-field seismic events associated with the Great Sumatran Fault. The synthetic time histories were obtained by standard wave matching technique, where design response spectra were used as input. The final time histories were obtained by trial and matching with target time history. In the present paper, three ground motions are referred as PGA-1 (0.022g), PGA-2(0.07g), and PGA-3 (0.1g), respectively.

2.2 Soil–Pile Response

Figure 3a, b shows the acceleration time histories computed at the clay surface and top of the raft. For this numerical simulation, solid stainless steel piles with added mass were used. The model was subjected to the ground motion of PGA-3. By comparing the computed histories and corresponding response spectra at the clay surface and top of the raft with those of the input ground motion, it is evident that the amplification of ground motion occurred in both the clay and the structure as the seismic waves propagate upwards. However, despite being at the same elevation, there are differences noted between the acceleration histories computed at the clay and raft, which suggest that the raft does not move in tandem with the ground. Figure 3c is replotted in Fig. 3d with the amplification of the input ground motion (PGA-3) obtained by normalizing the spectral acceleration at the clay and raft with respect to the base response.

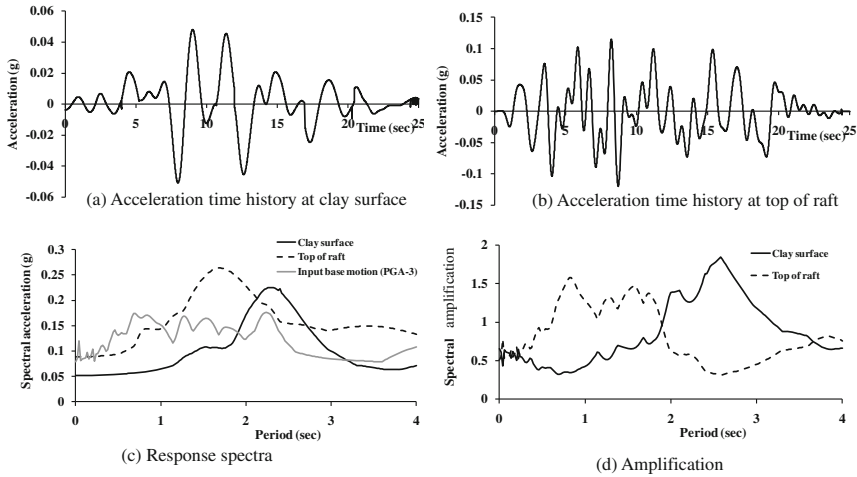


Fig. 3 Acceleration time histories, response spectra, and amplification

To measure the bending moment developed along the pile length, 3-noded beam elements were introduced along the centerline of the pile. The flexural rigidity of the beam was chosen as 10^6 times less than that of the pile so that the beam deformed freely without interfering with the structural response of the pile. The actual bending moment was obtained by multiplying computed beam moments by the scaling factor of 10^6 . Figure 4 shows that the maximum moment occurs near the pile-head reducing along the pile length to very small value near the pile tip.

2.3 Formulation of Dimensionless Parameters

In the present study, five dimensionless groups involving different parameters are identified as follows:

- (i) Stiffness ratio (T_p/T_s) is the ratio of the time period of the superstructure without the soil around it to that of the time period of the soil without any superstructure.

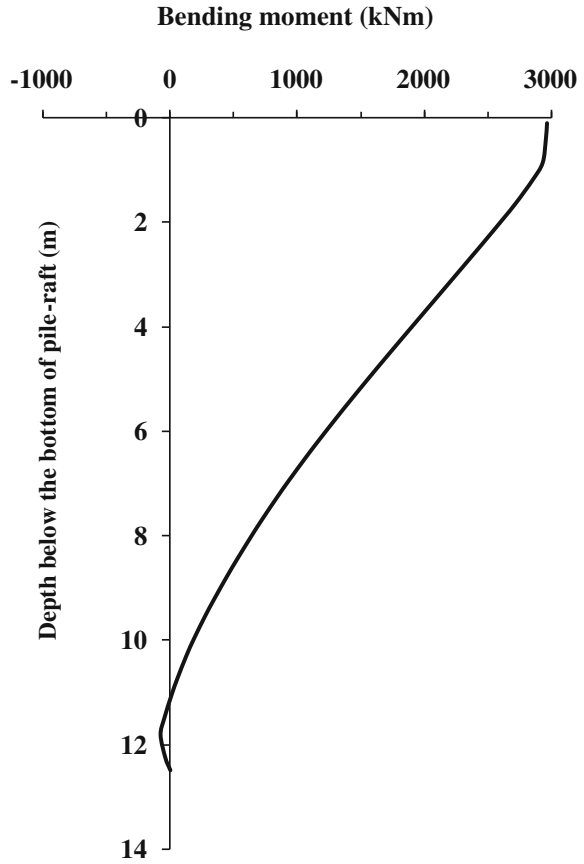
Time period of the superstructure is given by,

$$T_p = 2\pi \sqrt{\frac{mL_p^3}{3E_p I_p}} \tag{1}$$

where L_p is the length of pile, E_p is the modulus of elasticity, I_p is the moment of inertia, and m is the superstructure mass.

The time period of the soil layer is given by,

Fig. 4 Typical maximum bending moment profiles



$$T_s = \frac{4h}{\sqrt{\frac{G}{\rho}}} \tag{2}$$

where h is the height of the soil layer, G is the shear modulus of the soil layer, and ρ is the density of the soil layer.

- (ii) PGA is the peak ground acceleration of the base excitation expressed in terms of acceleration due to gravity (g).
- (iii) Mass ratio $\left(\frac{m}{\rho r_p^3}\right)$ is the ratio of mass of the superstructure to equivalent mass of soil. r_p is the radius of pile.
- (iv) Frequency ratio (f_b/f_0) where f_b is the predominant frequency of the input ground motions and $f_0 (= 1/T_s)$ is the natural frequency of the clay layer.
- (v) Slenderness ratio (L_p/d) is the ratio of the length of the pile to the diameter of the pile.

2.4 Parametric Study

A total of 27 numerical simulations involving three different pile types, super-structural masses and ground motions were carried out to establish semiempirical formulations for amplification at clay surface, top of raft, and maximum bending moment in pile.

Amplification at Clay Surface (A_s)

A detail regression analysis shows that the amplification at clay surface can be expressed as an exponential function (Fig. 5) of above-mentioned dimensionless groups as shown in Eqs. 3a and b.

$$A_s = 1.228 \times e^{57802x} \tag{3a}$$

$$x = \left(\frac{T_p}{T_s}\right)^{0.4} \times (PGA)^7 \times \left(\frac{m}{\rho r_p^3}\right)^{0.05} \times \left(\frac{f_b}{f_0}\right)^{0.6} \tag{3b}$$

It can be noted that the amplification at the clay surface primarily depend on PGA. It is also observed that the amplification at the clay surface increase with the decrease in clay stiffness.

Amplification at Top of Raft (A_r)

Amplification at the top of raft are expressed as a function of the amplification at the clay surface. Figure 6 shows the results of the regression analysis as follows:

$$A_r/A_s = 1.991 \times (A_s)^{-0.93} \tag{4}$$

From Eq. 4, it is noted that the amplification at the top of raft increase with the increase in the amplification at the clay surface.

Fig. 5 Semiempirical relationship for amplification at clay surface

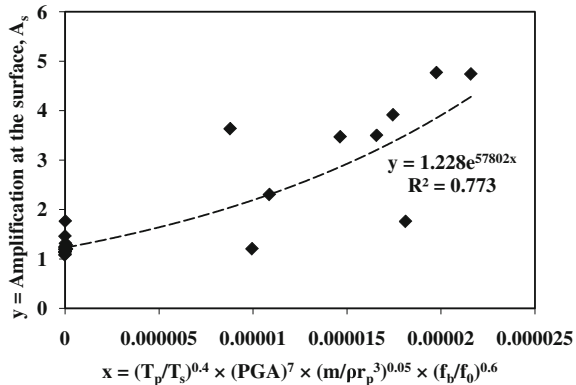


Fig. 6 Semiempirical relationship for amplification at the top of raft

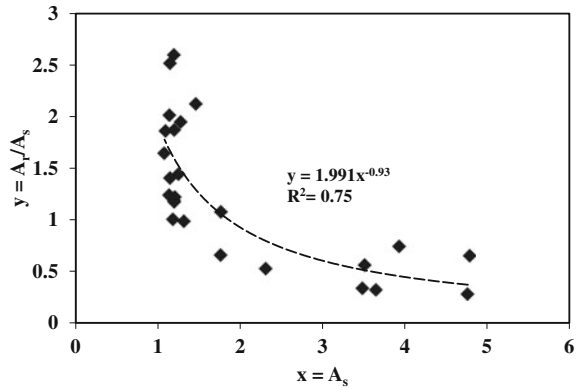
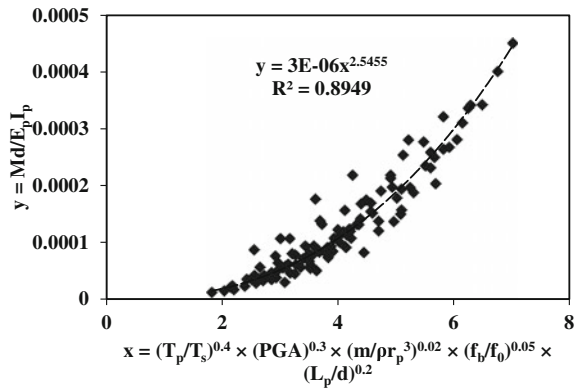


Fig. 7 Semiempirical relationship for maximum bending moment developed along the length of pile



Maximum Bending Moment Developed Along the Length of the Pile

The maximum moment is represented as a dimensionless formulation, $Md/E_p I_p$ where M is the maximum moment, d is the diameter of the pile, $E_p I_p$ is the flexural rigidity of the pile. The semiempirical formulation of the maximum bending moment is obtained by regression analysis (Fig. 7) is as follows:

$$\frac{M_d}{E_p I_p} = 3 \times 10^{-6} \times \{z\}^{2.545} \tag{5a}$$

$$z = \left(\frac{T_p}{T_s}\right)^{0.4} \times (PGA)^{0.3} \times \left(\frac{m}{\rho r_p^3}\right)^{0.02} \times \left(\frac{f_b}{f_0}\right)^{0.05} \times \left(\frac{L_p}{d}\right)^{0.2} \tag{5b}$$

Equations 5a and b suggests that the maximum bending moment increases with the pile modulus, peak ground acceleration, and superstructural load.

2.5 Validation of the Proposed Formulations

Preceding discussion shows that the clay and pile response can be represented as semiempirical functions of dimensionless groups. The responses computed from the proposed relationships are compared with the results reported in the previous studies.

Comparison with the Centrifuge Tests Results by Banerjee (2010)

Banerjee (2010) reported a series of shaking table experiments conducted using geotechnical centrifuge at National University of Singapore. Input earthquake motions and the soil types are used as the same as that considered in the numerical simulations. The accelerometers and strain gauges were used to measure acceleration time histories and bending moments, respectively. Figure 8a presents the comparison of the results computed from the proposed semiempirical relationship with the results obtained from the centrifuge tests for the amplification at the clay surface. The figure shows that, despite the uncertainties involved in the centrifuge tests, the predicted results matched the test results with reasonable accuracy. Figure 8b shows the comparison between the computed and measured amplification at the top of raft. The figure shows that the proposed correlations compare satisfactorily PGA-2 (0.07g) and PGA 3 (0.1g), whereas the centrifuge results obtained from test with ground motion of PGA-1 (0.022g) tend to deviate from the prediction. However, the ground motion with PGA of 0.022g is too small to be a concern in the context of amplification.

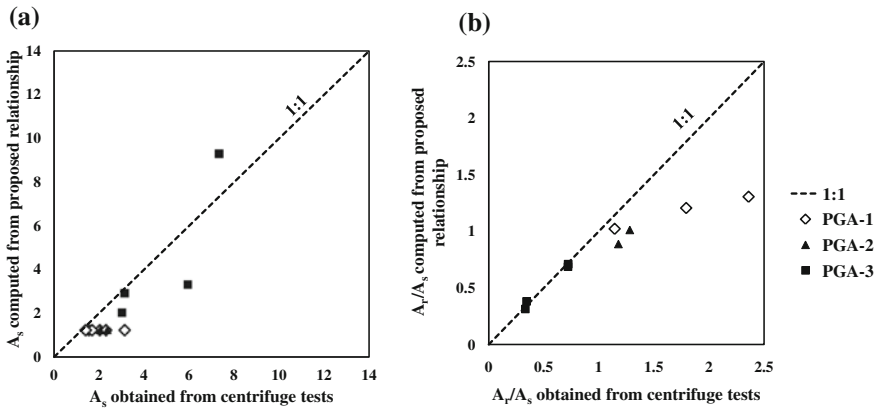


Fig. 8 Comparison of amplification at the **a** clay surface and **b** top of raft computed from proposed relationship with that obtained from centrifuge tests (Banerjee 2010)

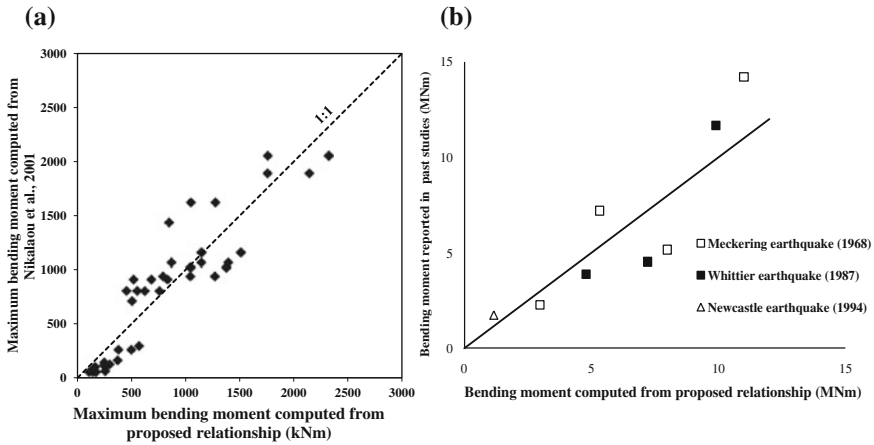


Fig. 9 Comparison between bending moments computed using proposed relationship with **a** Nikolaou et al. (2001) and **b** Poulos and Tabesh (1996)

Comparison with the Semiempirical Relationship Proposed by Nikolaou et al. (2001)

Nikolaou et al. (2001) developed a semiempirical relationship for maximum bending moment in piles embedded in layered soils (Eq. 6).

$$\max M \approx 0.042a_s\rho_1h_1d^3\left(\frac{l}{d}\right)^{0.3}\left(\frac{E_p}{E_1}\right)^{0.65}\left(\frac{V_1}{V_2}\right)^{-0.5} \quad (6)$$

where a_s is the free-field acceleration, ρ_1 is the density of topsoil (soil layer 1), h_1 is the height of the layer 1, l/d is the slenderness ratio of the pile, E_p is the modulus of elasticity of pile, E_1 is the modulus of elasticity of layer 1, V_1 and V_2 are the shear wave velocities of layer 1 and 2, respectively. It can be observed from Fig. 9a that the agreement between the proposed correlation and the formulation by Nikolaou et al. (2001) is fairly good. The slight deviations that is observed may be attributed to the effect of superstructure mass, which is not taken into account in the formulation by Nikolaou et al. (2001).

Comparison with the Analysis Reported by Poulos and Tabesh (1996)

Poulos and Tabesh (1996) presented an analysis for the seismic response of single piles ignoring inertia of piles. Figure 9b plots the bending moments computed from the proposed relationship along with Poulos’ analysis. Figure shows that, in general, good agreement is achieved between the two analyses.

3 Concluding Remarks

The foregoing discussion suggests that the three-dimensional numerical analysis can be very effective to model complex soil–pile systems. It can also be found that the response of clay and piles subjected to seismic loading is affected by various factors such as pile modulus, soil modulus, slenderness ratio, natural frequencies of clay layer and pile-raft, superstructure mass, density of the soil and peak ground acceleration. The developed correlations are favorably validated with the previously published experimental results (Banerjee 2010) as well as the numerical analysis reported by Nikolaou et al. (2001) and Poulos and Tabesh (1996). However, it should be noted that the developed correlations are valid for fixed-head, end-bearing piles in homogenous clay. Further details of this study can be found in following literatures:

1. S Banerjee, M Joy & D Sarkar (2016). Parametric study and centrifuge-test verification for amplification and bending moment of clay–pile system subjected to earthquakes. *Geotechnical and Geological Engineering* 34 (6), 1899–1908.
2. S Banerjee & O N Shirole (2014). Numerical analysis of piles under cyclic lateral load. *Indian Geotechnical Journal* 44 (4), 436–448.
3. S Banerjee, S H Goh & F H Lee (2014). Earthquake-induced bending moment in fixed-head piles in soft clay. *Géotechnique* 64 (6), 431–446.

References

- Banerjee, S., Goh, S. H., & Lee, F. H. (2007). Response of soft clay strata and clay-pile-raft systems to seismic shaking. *Journal of Earthquake and Tsunami*, 1(3), 233–255.
- Banerjee, S. (2010). *Centrifuge and numerical modelling of soft clay-pile-raft foundations subjected to seismic shaking (Ph.D. thesis)*. National University of Singapore.
- Dobry, R. (1982). Horizontal stiffness and damping of single piles. *Journal of Geotechnical and Geoenvironmental Engineering*, 108(GT3), 439–456.
- Goh, T. L. (2003). Stabilization of an excavation by an embedded improved soil layer. Singapore: Ph.D. Thesis, National University of Singapore.
- Nikolaou, S., Mylonakis, G., Gazetas, G., & Tazoh, T. (2001). Kinematic pile bending during earthquakes: Analysis and field measurements. *Geotechnique*, 51(5), 425–440.
- Novak, M. (1974). Dynamic stiffness and damping of piles. *Canadian Geotechnical Journal*, 11(4), 574–598.
- Poulos, H. G., & Tabesh, A. (1996). Seismic response of pile foundations—some important factors. In *Proceedings of 11th WCEE paper no. 2085*.
- Shen, W. Y., & The, C. I. (2004). Analysis of laterally loaded piles in soil with stiffness increasing with depth. *Journal of Geotechnical and Geoenvironmental Engineering ASCE*, 130(8), 179–215.
- Vucetic, M., & Dobry, R. (1991). Effect of soil plasticity on cyclic response. *Journal of Geotechnical Engineering ASCE*, 117(1), 89–107.
- Yu, Y., & Lee, F. H. (2002). Seismic response of soft ground. In *Proceedings of physical modeling in geotechnics-ICPMG'02* (pp. 519–524). St. John's, Canada.
- Zhang, F., Kimura, M., Nakai, T., & Hoshikawa, T. (2000). Mechanical behavior of pile foundations subjected to cyclic lateral loading up to the ultimate state. *Soils and Foundations*, 40(5), 1–17.